

# Parametric Versus Nonparametric Transfer Function Estimation of Cerebral Autoregulation from Spontaneous Blood-Pressure Oscillations

Michael Jachan · Matthias Reinhard ·  
Linda Spindeler · Andreas Hetzel · Björn Schelter ·  
Jens Timmer

Published online: 28 May 2009  
© Springer Science+Business Media, LLC 2009

**Abstract** Cerebral autoregulation (CAR) is a control mechanism of the brain keeping cerebral blood flow constant albeit the arterial blood pressure varies. Impaired CAR may be associated with an increased risk of cerebral ischemic events in patients with obstructive cerebrovascular disease. Spontaneous blood pressure oscillations are analyzed using a nonparametric and two parametric transfer function estimators, i.e. the autoregressive-moving-average model with exogenous inputs or the vector-autoregressive model. Performance of the methods was compared using data from patients with unilateral stenosis or occlusion. We also analyzed reproducibility by comparing partitions of the data with data from other patients which have been measured twice. Results show that there is no significant difference between methods (ANOVA,  $p > 0.27$ ), and that CAR measurements can be performed reproducibly (Kendall's  $\tau$ ,  $p < 0.0016$ ) by all three methods. In conclusion, CAR measurements by means of spontaneous oscillations can be obtained stably and the presented parametric approaches can serve for future online application of CAR measurement.

**Keywords** Cerebral autoregulation · Spontaneous blood pressure oscillations · ARMAX, VAR · Reproducibility

## Introduction

Dynamic cerebral autoregulation (CAR) tries to hold the blood supply of the brain constant albeit the arterial blood pressure (ABP) varies (Panerai 1998; Panerai 2008). Noninvasive diagnosis of the human CAR system, especially of patients with cerebrovascular disease, may aid in understanding the pathophysiology of these conditions and to identify high risk patients. Noninvasive monitoring of CAR can be based on the physiological oscillations cerebral blood flow velocity (CBFV) and ABP. Basic CAR functionality can be analyzed by investigating the response of CBFV to artificial, i.e. experimental changes in mean ABP. Newer types of experimental setups exhibit an intrinsic periodic character, thus making the use of *transfer function analysis* possible. Such a method to induce periodic alternations of ABP and cerebral perfusion is regular slow breathing at 6 cycles/min called the deep breathing method (Diehl et al. 1995). A spectral peak at 0.1 Hz in the transfer function describes in which way the basic rhythms of ABP and CBFV are related in amplitude and phase. An existing phase shift (30–90°) thereby indicates a functioning CAR mechanism while a diminishing phase shift (below 20–30°) speaks for an impaired CAR system. However, acutely ill subjects might not be able to perform the deep breathing experiment. In this situation, also spontaneous respiratory-induced oscillations (SPO) in ABP can be used to quantify CAR functionality. Such SPOs can occur in different frequency bands: A pronounced peak at the pulse frequency around 1 Hz (P-waves), a broad peak at the respirational frequency of 0.3 Hz (R-waves) and a

M. Jachan (✉) · L. Spindeler · B. Schelter · J. Timmer  
Center for Data Analysis and Modeling (FDM), Freiburg  
University, Eckerstr. 1/FDM, 79104 Freiburg, Germany  
e-mail: michael.jachan@fdm.uni-freiburg.de

M. Jachan · M. Reinhard · A. Hetzel  
Department of Neurology, University Hospital of Freiburg,  
Freiburg, Germany

M. Jachan · L. Spindeler · B. Schelter · J. Timmer  
Bernstein Center for Computational Neuroscience (BCCN),  
Freiburg University, Freiburg, Germany

J. Timmer  
Freiburg Institute for Advanced Studies (FRIAS), University of  
Freiburg, Albertstr. 19, 79104 Freiburg, Germany

peak in the low-frequency region around 0.1 Hz (M-waves). Here, the average phase of M-waves in the band 0.06–0.12 Hz is used as the CAR-related parameter Zhang et al. (1998). The SPO method is very elegant and promising Diehl et al. (1998), because it works without any external manipulation of the subject. However, it is very challenging from an analytical point of view because no clear spectral peak is present.

This study aims to develop CAR analysis approaches based on parametric transfer function estimation utilizing either an autoregressive-moving-average model with exogenous inputs (ARMAX) or a vector-autoregressive model (VAR) model. Parametric approaches have the particular advantages that less parameter estimates are necessary than with a nonparametric approach, and also that no spectral smoothing is necessary.

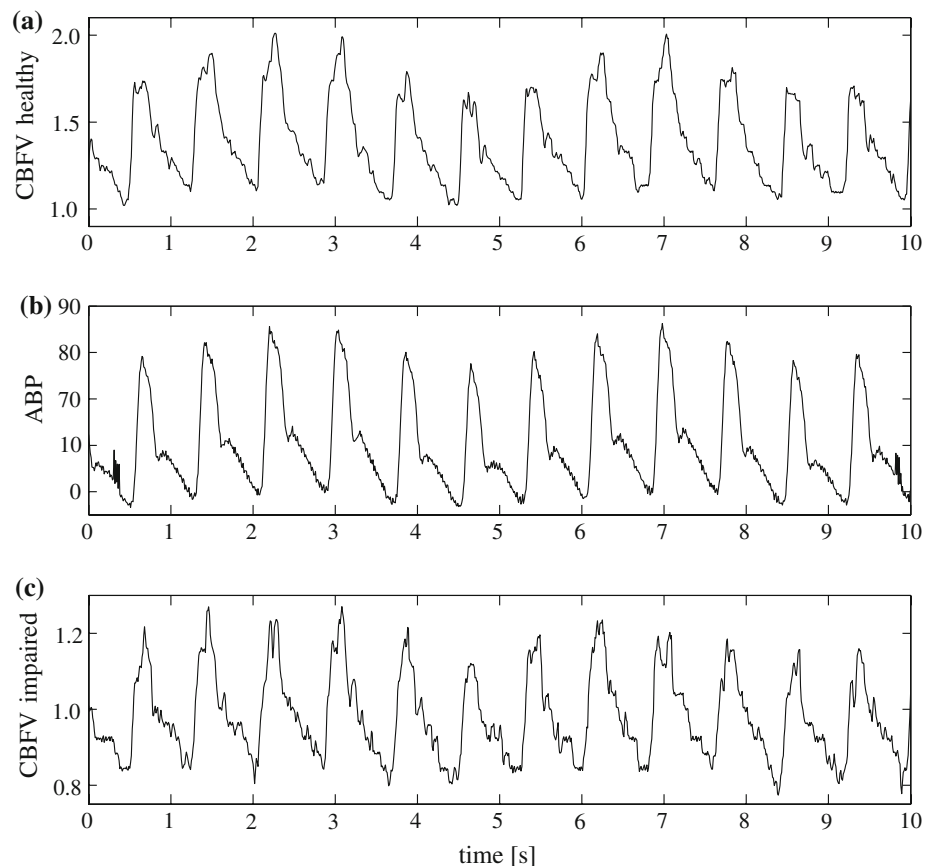
## Methods

### Transfer Function Estimation

The physiological measurements are regarded as discrete-time weakly stationary processes (Brockwell and Davis

1998), whose means have been subtracted. The ABP is denoted by  $x_{\text{ABP}}(t)$  and the two channels of the CBFV are  $y_{\text{CBFV}}^{(k)}(t)$ ,  $k = r, l$ , where  $r$  and  $l$  stand for right and left, respectively. The time index  $t$  is limited by a given recording time  $T$ , which together with the sampling frequency determines the number of samples  $N = T f_s$ . A typical signal portion of an unilaterally impaired patient is depicted in Fig. 1. We model the ABP to be related to each of the CBFV channels by a causal linear system, i.e. the *transfer function*  $H^{(k)}(\omega)$ , where  $\omega \in [0, \pi]$  is the relative frequency. An established nonparametric method is reviewed firstly, which serves as a reference method. From an observation of several minutes, one can estimate the transfer function by means of cross-spectral analysis based on the *smoothed periodogram estimator*. For this spectral estimator a smoothing kernel has to be designed, it determines a trade-off between spectral resolution and estimation variance. Here, a triangular window with a half width of  $h = 8$  frequency bins Reinhard et al. (2003) is utilized. The cross-spectrum estimates of  $x_{\text{ABP}}(t)$  and  $y_{\text{CBFV}}^{(k)}(t)$  are denoted as  $\hat{P}_{\text{ABP},k}(\omega)$  and the auto-spectrum estimate of each signal is given by e.g.  $\hat{P}_{\text{ABP}}(\omega)$ . A nonparametric, smoothed periodogram-based estimator of the transfer function can be derived as Brockwell and Davis (1998), Reinhard et al. (2003)

**Fig. 1** Exemplary data set consisting of three time series. **a** Cerebral blood flow velocity of the healthy side, **b** arterial blood pressure, and **c** cerebral blood flow velocity of the impaired side



$$\hat{H}_{\text{sm.p.}}^{(k)}(\omega) \triangleq \frac{\hat{P}_{\text{ABP},k}^*(\omega)}{\hat{P}_{\text{ABP}}(\omega)}, \quad k = r, l. \quad (1)$$

From the transfer function estimate, one can extract the phase parameter as the average phase in the M-band as

$$\psi_{\text{sm.p.}}^{(k)} \triangleq \frac{1}{0.06\text{Hz}} \int_{0.06\text{Hz}}^{0.12\text{Hz}} \arg \left\{ \hat{H}_{\text{sm.p.}}^{(k)} \left( 2\pi \frac{f}{f_s} \right) \right\} df, \quad k = r, l. \quad (2)$$

$\psi_{\text{sm.p.}}^{(k)}$  has proven to be a relevant CAR analysis parameter (Zhang et al. 1998). Note that a phase estimate is reliable only if the according coherence is significantly larger than zero (Brockwell and Davis 1998). As a criterion the significance level ( $\alpha = 5\%$ ) of the coherence is used, and only frequency bins with a significant coherence will be included in the phase averaging (2).

### Transfer Function Estimation Using ARMAX Modeling

In this section the transfer function estimation will be performed using two parametric ARMAX( $P_k, Q_k$ ) models (Ljung 1987; Panerai et al. 2001, 2003; Liu and Allen 2002; Liu et al. 2005). Again, the input signal to each ARMAX model is the ABP signal  $x_{\text{ABP}}(t)$  and the output signals are right respectively left CBFV signals  $y_{\text{CBFV}}^{(k)}(t)$ ,  $k = r, l$ . The ARMAX models are defined by the difference equation

$$y_{\text{CBFV}}^{(k)}(t) = - \sum_{p=1}^{P_k} a_p^{(k)} y_{\text{CBFV}}^{(k)}(t-p) + \sum_{q=0}^{Q_k} b_q^{(k)} x_{\text{ABP}}(t-q), \quad k = r, l, \quad (3)$$

where  $a_p^{(k)}$ ,  $p = 1, \dots, P_k$  are autoregressive (AR) parameters and  $b_q^{(k)}$ ,  $q = 0, \dots, Q_k$  are moving-average (MA) parameters.  $P_k$  respectively  $Q_k$  are model orders of the right and left AR respectively MA models. By applying the Fourier transform to (3), one can find the transfer functions, which are completely described by the ARMAX parameters. After the model parameters and the orders have been estimated, an ARMAX-based transfer function estimator is obtained as (cf. Eq. 1)

$$\hat{H}_{\text{ARMAX}}^{(k)}(\omega) \triangleq \frac{\sum_{q=0}^{Q_k} \hat{b}_q^{(k)} e^{-i\omega q}}{\sum_{p=0}^{P_k} \hat{a}_p^{(k)} e^{-i\omega p}}, \quad k = r, l, \quad (4)$$

where  $i$  is the imaginary unit and  $a_0^{(k)} = 1$ . A broad variety of estimation methods for ARMAX models are known, e.g. the least-squares method (Ljung 1987). Order estimation can be performed with e.g. the Bayesian information criterion (BIC), which is given as (Choi 1992)

$$\text{BIC}(P, Q) = \log \sigma_{P,Q}^2 + \frac{P+Q}{N} \log N,$$

where  $\sigma_{P,Q}^2$  is the variance of the error signal, i.e. the difference between  $y_{\text{CBFV}}^{(k)}(t)$  and  $x_{\text{ABP}}(t)$  filtered by the ARMAX( $P, Q$ ) model. We prefer the BIC over the AIC, because it delivers asymptotically consistent estimates. Once the ARMAX model has been identified, the average phase  $\psi_{\text{ARMAX}}^{(k)}$  in the M-band 0.06–0.12 Hz can be found by plugging (4) into (2).

For the estimation of the significance level of the coherence estimated by the ARMAX model we propose to use a bootstrap technique. We compute AR(30) fits of  $y_{\text{CBFV}}^{(r)}(t)$ ,  $y_{\text{CBFV}}^{(l)}(t)$ , and  $x_{\text{ABP}}(t)$  separately, and we computed each of the three innovations sequences by inverting each of the AR(30) models. By shuffling these estimated innovations sequences, we generate new stimuli for each of the innovations models. In this way numerous realizations of the  $\tilde{y}_{\text{CBFV}}^{(k)}(t)$  and  $\tilde{x}_{\text{ABP}}(t)$  can be synthesized, which do not show any coherence. The distribution of these coherence estimates is thus a distribution under the null hypothesis that no coherence is present, and the 95% quantile serves as a significance level.

### Transfer Function Estimation Based on Vector-AR Innovations Modeling

The above CAR methodologies use separate models for the right and left branches. Next, a multivariate modeling technique, which regards all three physiological time series as output processes of a VAR model is presented. The models' output process is defined to be the zero-mean process

$$z(t) \triangleq \begin{bmatrix} y_{\text{CBFV}}^{(r)}(t) \\ y_{\text{CBFV}}^{(l)}(t) \\ x_{\text{ABP}}(t) \end{bmatrix}^T \in \mathbb{R}^3$$

and the input is a stationary white innovations process  $e(t) \in \mathbb{R}^3$ , which has matrix covariance function  $\mathbf{R}_e(m) = \Sigma_e \delta(m)$ , where  $\delta(m)$  is the Dirac function,  $m$  is the time lag, and  $\Sigma_e = \mathcal{E}\{e(t)e^T(t)\}$ . The unaccessible process  $e(t)$  is a driving noise for the VAR model and is an expression for the remaining modeling error. The VAR model equation is (Hannan and Deistler 1988)

$$z(t) = - \sum_{p=1}^{P_{\text{VAR}}} \mathbf{A}_p z(t-p) + e(t), \quad (5)$$

where  $\mathbf{A}_p, p = 1, \dots, P_{\text{VAR}}$  are the  $3 \times 3$  AR parameter matrices and  $P_{\text{VAR}}$  is the VAR model order. The transfer functions  $\hat{H}_{\text{VAR}}^{(k)}(\omega)$  linking CBFV to ABP (cf. Eqs. 1, 4) can be found by inspecting the spectral density matrix of the VAR model defined as  $\mathbf{S}_z(\omega) \triangleq \mathbf{A}^{-1}(\omega) \Sigma_e \mathbf{A}^{-H}(\omega)$ , with the matrix polynomial  $\mathbf{A}(\omega) \triangleq \sum_{p=0}^{P_{\text{VAR}}} \mathbf{A}_p e^{-i\omega p}$ , where  $\mathbf{A}_0 = \mathbf{I}$ . After the parameter matrices  $\mathbf{A}_p$  and  $\Sigma_e$  have been estimated, one can compute the auto- and cross spectral matrix respectively its components

$$\hat{\mathbf{S}}_z(\omega) = \begin{bmatrix} \hat{S}_r(\omega) & \hat{S}_{r,l}(\omega) & \hat{S}_{r,ABP}(\omega) \\ \hat{S}_{l,r}(\omega) & \hat{S}_l(\omega) & \hat{S}_{l,ABP}(\omega) \\ \hat{S}_{ABP,r}(\omega) & \hat{S}_{ABP,l}(\omega) & \hat{S}_{ABP}(\omega) \end{bmatrix}.$$

Analogue to (1), the VAR-based estimator of the transfer functions relevant for CAR modeling is defined as

$$\hat{H}_{VAR}^{(k)}(\omega) \triangleq \frac{\hat{S}_{ABP}^*(\omega), k(\omega)}{\hat{S}_{ABP}(\omega)}, \quad k = r, l, \quad (6)$$

where only the lower three elements of  $\hat{\mathbf{S}}_z(\omega)$  have been used. For VAR models, also a broad variety of parameter estimators are available (Kay 1988) and the BIC can serve for order estimation. From Eq. 6, the phase parameters  $\psi_{VAR}^{(k)}$  (cf. Eq. 2) can be estimated. We also base the validity of the phase estimate incorporating the VAR model on the estimated coherency, whose significance level is estimated by the same bootstrap approach as for the ARMAX model.

### Analysis of Model Complexity

The size of a modeling approach can be quantified by its number of real-valued parameters  $M$ . The more parameters have to be estimated from a given sample, the higher the estimation variance becomes. Thus, the ratio parameters  $M$  to data size should be kept small. In our case,  $M$  is the number of real-valued parameters, which is needed to compute the phases of right and left transfer functions *in the interesting frequency range*. The number of relevant frequency bins depends on the frequency resolution given by  $\Delta f = f_s/N$ , which is constant if the measurement time  $T$  is fixed. Let us now compute  $M$  for all three discussed modeling approaches. For the smoothed periodogram method both cross-spectral estimates  $\hat{P}_{ABP,k}(\omega)$  have to be considered, because only they carry the phase information. The number of relevant complex-valued parameters in the M-band is  $\left\lceil \frac{0.06}{\Delta f} + 1 + 2h \right\rceil$ , thus one obtains  $M_{sm.p.} = 2 \left\lceil \frac{0.06}{\Delta f} + 1 + 2h \right\rceil$  per side, which is inversely proportional to  $\Delta f$ . The transfer function estimates from the ARMAX approach (4) at any frequency are represented by all real-valued estimated ARMAX parameters, thus  $M_{ARMAX} = P_r + Q_r + P_l + Q_l + 2$ . Finally, the VAR approach (6) needs  $M_{VAR} = 9P_{VAR} + 6$  real-valued model parameters for describing both transfer functions, where six parameters are for the Hermitian matrix  $\Sigma_e$ .

### Patient Collectives, Data Acquisition and Processing

The current methods were applied to a group of previously studied patients with severe (>70%) uni- or bilateral internal carotid artery stenosis or occlusion (Reinhard et al.

2003). Measurements were performed with the patients in a supine position with an inclination of 50° of the upper body. Cerebral blood flow velocity (CBFV) was measured in both middle cerebral arteries by transcranial Doppler sonography (DWL-Multidop-X ©, Sipplingen, Germany) with 2 MHz transducers attached to a headband. Non-invasive recordings of arterial blood pressure (ABP) were obtained with a servo-controlled finger plethysmograph (Finapres © 2300, Ohmeda, Englewood CO) with the subjects right hand positioned at heart level. For the present analysis, spontaneous oscillations of ABP and CBFV during a resting period of 10 min were used. All data were sampled at 100 Hz and for further analysis, the sampling rate was reduced to 2.5 Hz incl. appropriate lowpass filtering. From the raw data a segment of  $T = 400$  s has been selected and reviewed for measurement artifacts. For the estimation of the ARMAX models the least-squares method (Ljung 1987) including the BIC for order estimation was implemented. VAR estimation has been performed by using a least-squares method from Neumaier and Schneider (2001) and Schneider and Neumaier (2001) including the BIC as order estimation criterion.

The results which will be presented in the next section have been obtained on two different patient collectives. On the first set of patients, called data set I, a comparison of the three discussed model types in terms of statistical equivalence and model complexity was performed. We also assess short-term reproducibility on data set I. From  $n_0 = 91$  unilateral impaired patients (mean age 65, standard deviation 10 years, 35–85 years, 14 female) we obtained data from healthy sides as well as from impaired sides. Sides which did not show coherence significantly larger than zero assessed by the 95% confidence interval of the coherence at at least one frequency bin between 0.06 and 0.12 Hz have not been included in the analysis. We then analyze long-term reproducibility of all three estimators separately by means of a collective of consecutive patient measurements, called data set II. Forty four patients (mean age 71, standard deviation 10 years, 43–84 years, 6 female) have been reexamined after a mean interval of 2.5 months, range 6 months, where the degree of stenosis was confirmed to be unchanged beforehand.

## Results

### Inter-Method Agreement

For healthy and impaired sides, we tested the phases from all three estimation methods for differences in the mean by a two-way ANOVA for repeated measurements from data set I (cf. Table 1). In Figs. 2 and 3 the scatterplots for the healthy and for the impaired sides are shown. These figures

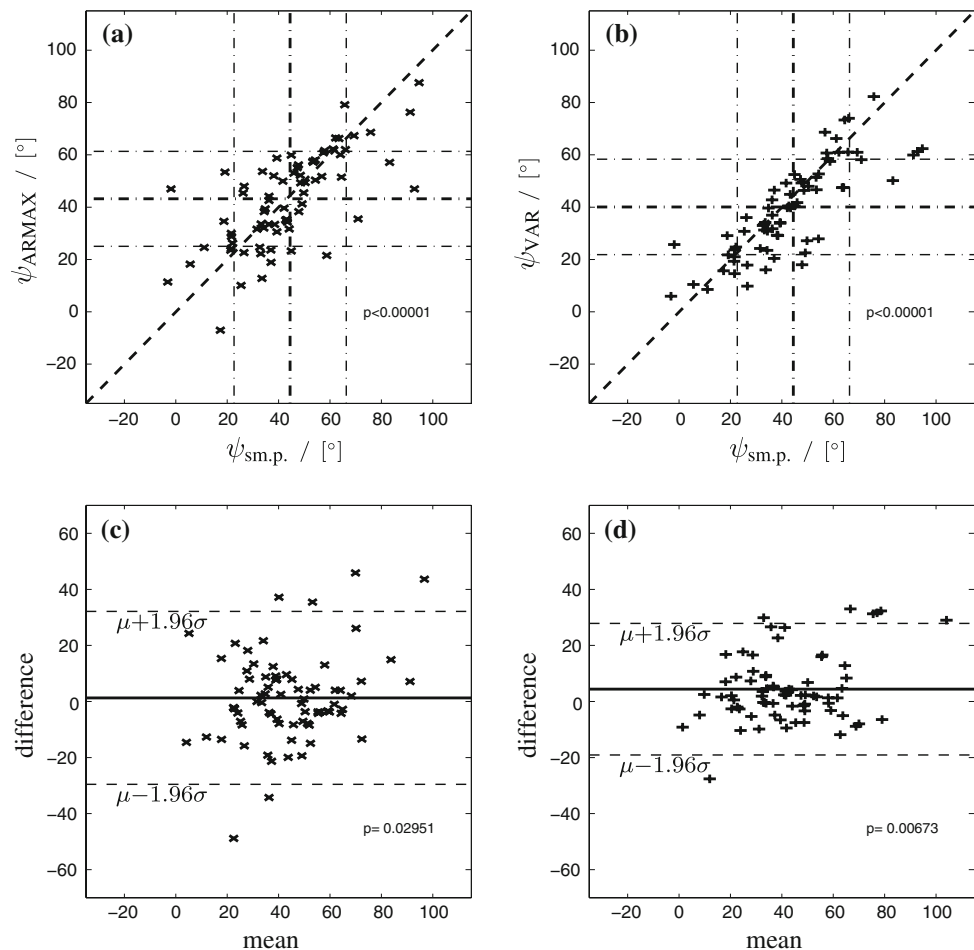
**Table 1** Statistical results for the inter-method comparison smoothed periodogram, ARMAX and VAR on data set I

Sides	Approach	$\psi$ $\mu \pm \sigma$	ANOVA, $p$ value	
			Inter-method	Healthy vs. impaired
Healthy	Smoothed per.	$43.2 \pm 23.3$	0.279	0.000133*
	ARMAX	$44.0 \pm 20.3$		
	VAR	$42.3 \pm 18.8$		
Impaired	Smoothed per.	$29.4 \pm 23.8$	0.450	
	ARMAX	$33.5 \pm 22.9$		
	VAR	$29.1 \pm 20.6$		

\* Significant differences

The phase was evaluated in the frequency range 0.06–0.12 Hz for all three methods and on the healthy and impaired sides separately. Columns 4 and 5 state the  $p$  values for the inter-method comparison and the comparison healthy versus impaired

**Fig. 2** Healthy side of data set I (maximum length  $N = 40,000$ ). *Top row* scatterplots of the parametric methods versus the smoothed periodogram method: **a** ARMAX versus smoothed periodogram, **b** VAR vs. smoothed periodogram.  $p$  values from Kendall's  $\tau$ . *Dashed-dotted lines* indicate the mean  $\pm$  variance of the marginal distributions. *Bottom row* Bland-Altman plots with the smoothed periodogram as a reference method: **c** ARMAX versus smoothed periodogram, **d** VAR versus smoothed periodogram. The *dashed lines* show the 95% confidence interval of the differences and the *solid line* indicated the bias.  $p$  values from linear regression difference versus mean

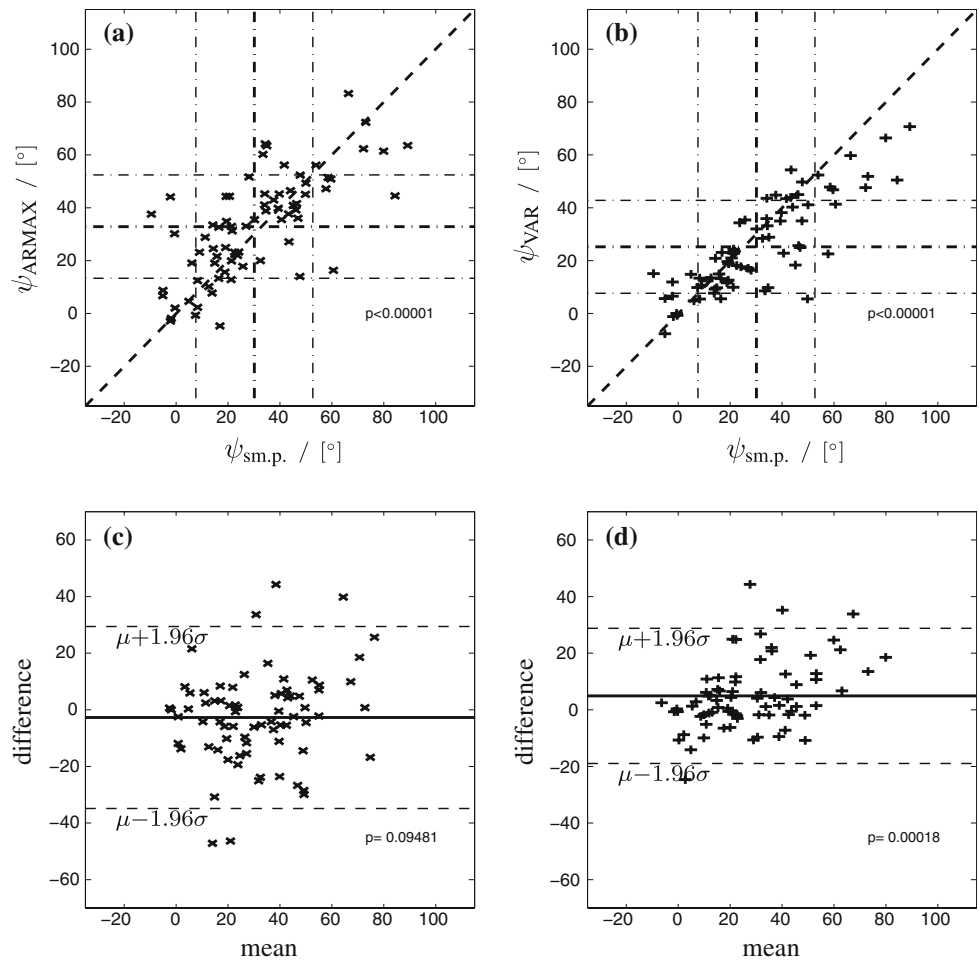


also show Bland-Altman plots, which are rotated scatterplots such that the mean value of both measurements are plotted against their difference. The mean of the phase estimate from the smoothed periodogram, the ARMAX, and the VAR approach are not significantly different (healthy side:  $p = 0.279$ , impaired side:  $p = 0.450$ , cf. Table 1). The healthy side shows a significant higher phase parameter than the impaired side for all three methods ( $p < 0.0002$ ). On average, the ARMAX model shows the

lowest complexity, i.e. the lowest  $\bar{M} = 20$ , while the smoothed periodogram method ( $\bar{M} = 164$ ) and the VAR method ( $\bar{M} = 80$ ) need more model parameters to describe the phase in the M-band.

We also present the same analysis for shorter signal blocks from data set I in Fig. 4. The VAR model is able to yield significant coherence estimates also for short data segments  $N \geq 12,000$ , while the ARMAX and the smoothed periodogram drop several patients for shorter  $N$  (cf. Fig. 4a).

**Fig. 3** Impaired side of data set I (maximum length  $N = 40,000$ ). *Top row* scatterplots of the parametric methods versus the smoothed periodogram method: **a** ARMAX versus smoothed periodogram, **b** VAR versus smoothed periodogram.  $p$  values from Kendall's  $\tau$ . *Dashed-dotted lines* indicate the mean  $\pm$  variance of the marginal distributions. *Bottom row* Bland-Altman plots with the smoothed periodogram as a reference method: **c** ARMAX versus smoothed periodogram, **d** VAR versus smoothed periodogram. The *dashed lines* show the 95% confidence interval of the differences and the *solid line* indicated the bias.  $p$  values from linear regression difference versus mean



For all three methods, the phase estimate (mean and standard deviation) do not depend on  $N$  (cf. Fig. 4b). Also the coefficient of variation, which is defined as  $CV = \sigma/\mu$  is stable for varying block length as depicted in Fig. 4c. The average model orders (Fig. 4d) and average model complexity  $\bar{M}$  (Fig. 4e) increase slowly with  $N$  for both parametric methods whilst for the smoothed periodogram it is constant.

**Measurement Reproducibility**

The proposed estimators have been applied to two consecutive signal portions of length  $N = 20,000$  of data set I and to both measurements of data set II ( $N = 40,000$ ) to analyze whether CAR can be measured in a reproducible manner. For the first setup we refer to short-term reproducibility and for the second setup we refer to long-term reproducibility. Only sides which showed significant coherence for both measurements have been included in the analysis. Scatterplots plots are presented in Fig. 5. For all three methods significant correlations between both measurements ( $p < 0.0016$ ) have been found by Kendall's rank correlation. For the data from data set I, i.e. short-term

reproducibility, the variability between measurements 1 and 2 are very low as depicted in Fig. 5d–f. For the measurements of data set II, i.e. long-term reproducibility, much more variability is present (cf. Fig. 5a–c). Also, the coefficients of variation are very similar for short-term reproducibility, while for long-term reproducibility they vary much more. This variability can be explained by several external influences, such as progress of the disease or changing condition of the subject. These influences are certainly not present in short-term reproducibility. However, even for long-term reproducibility a highly significant correlation between both measurements can be obtained.

**Discussion**

In this study, a nonparametric and two parametric transfer function estimators for the assessment of the dynamic cerebral autoregulation from noninvasive measurements of spontaneous oscillations were analyzed. Essentially, we could not find a difference in performance between the methods and we showed highly significant short-term and

**Fig. 4** Analysis of the estimators for increasing  $N$ . **a** Number of significant sides (solid: VAR, dashed: ARMAX, dashed-dotted: smoothed periodogram); **b** mean plus/minus standard deviation of phase estimate  $\psi$ ; **c** coefficients of variation; **d** mean plus standard deviation of model orders (diamonds:  $P$ , squares:  $Q$ , rings:  $P_{VAR}$ ); **e** average model complexity

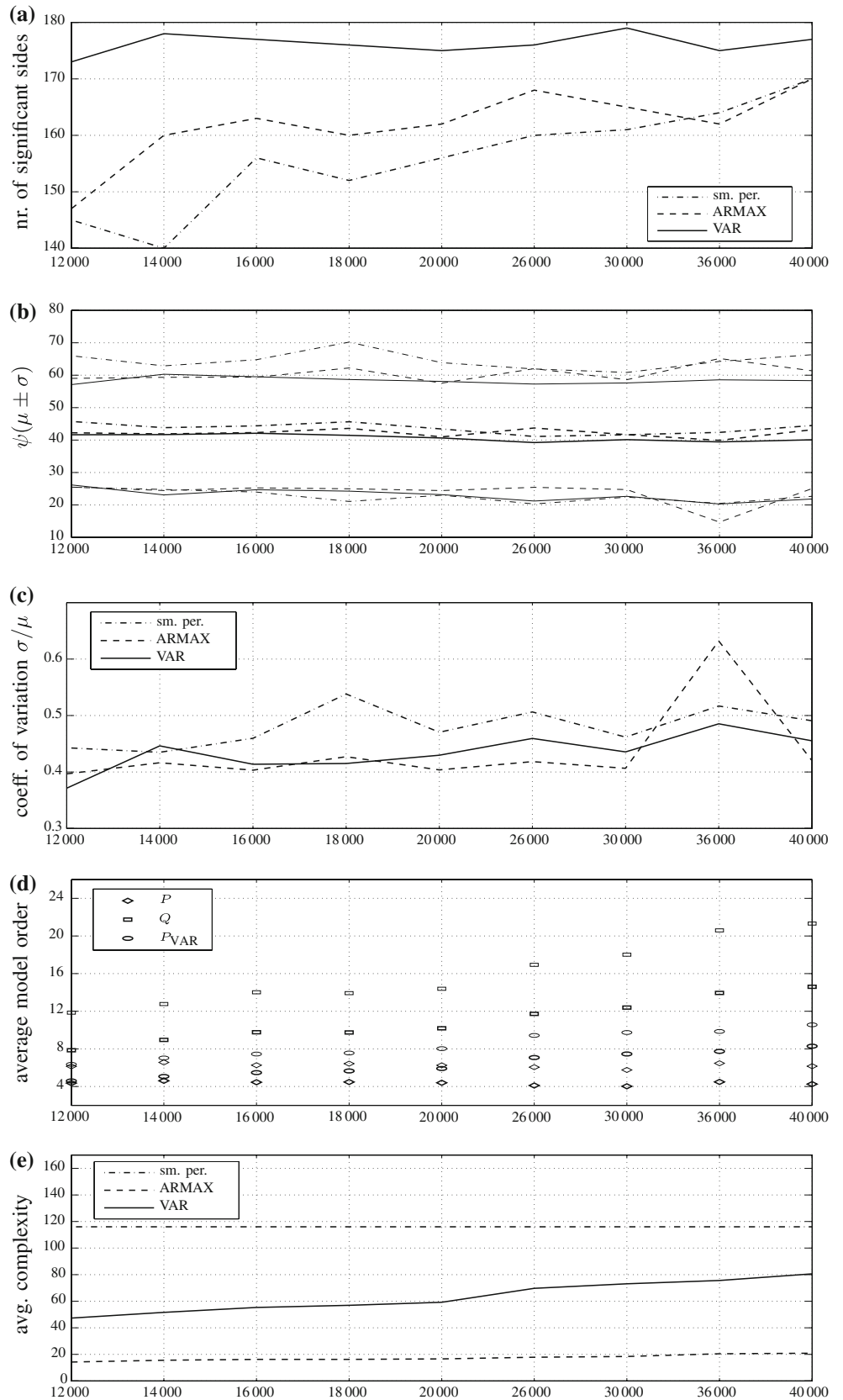
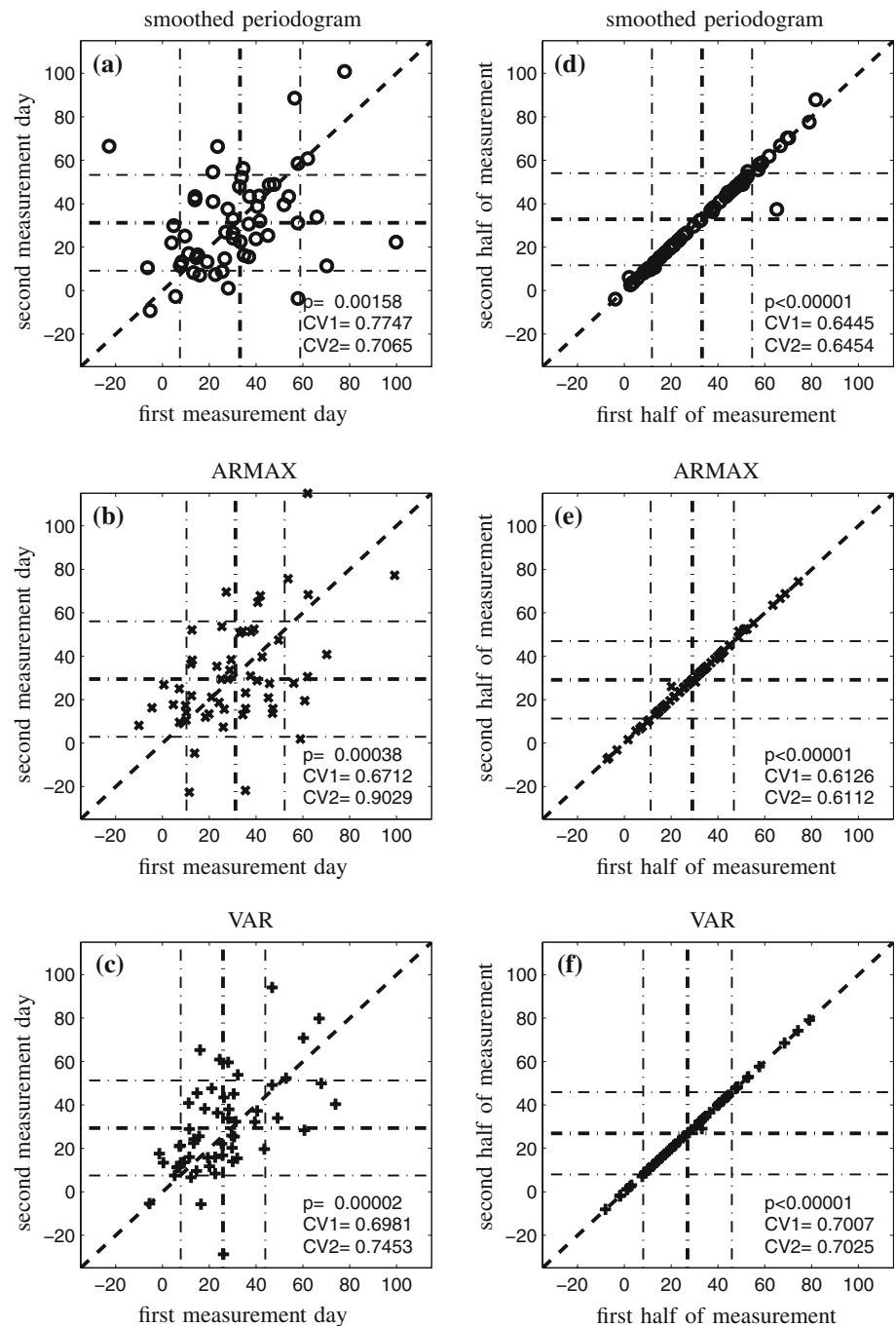


**Fig. 5** Repeated measurements. **a–c** on two separate days (data set II), **d–f** by splitting a given data block into two half (data set I). For the case with measurements on separate days (**a–c**) the reproducibility is much lower than for the second case (**d–f**) as the  $p$  values are much higher. The coefficient of variation  $CV = \sigma/\mu$  is stated in each subplot. However, for all cases highly significant correlations (Kendall's  $\tau$ ) have been obtained ( $p < 0.002$ )



long-term reproducibility for all three methods. Parametric models have also been applied in other fields related to cerebral hemodynamics. In Matsukawa and Wada (1997) a VAR model was utilized to analyze the feedback relationship between fluctuations in blood pressure and the heart rate, while in Panerai et al. (2001, 2003) an ARMAX model was used to assess CAR functionality. These studies demonstrated that physiological data can be modeled by parametric approaches and that several properties of the human feedback regulation related to hemodynamics can

be measured reliably. In contrast to the present study, the measurement setups were based on time-domain methods and not on frequency-domain methods, thus other parameters than the phase parameter as in here have been quantified. In Panerai et al. (2003) the authors considered the autoregulation index (ARI) (Tiecks et al. 1995) instead and reformulated it in terms of ARMA models. Also, a cardiac cycle averaging (R–R preprocessing) has been included and order estimation has not been performed on each single observation, but on an ensemble of data. It was

shown that the ARMA-ARI produces more stable estimates compared to the regular ARI. Parametric models have thus proven to be a valuable tool to analyze signals stemming from the human circulation system. Especially for CAR assessment they are able to deliver valid results for time- and frequency domain setups.

For a physiologically meaningful interpretation of the present data it is of importance that the blood pressure measured at the index finger is reasonably representing the blood pressure in the carotid artery. Differences in pulse pressure and to a lesser degree in mean blood pressure between the Finapres device and invasively recorded blood pressure in the aorta have been reported. These differences lead to small but significant differences in parameters that characterize dynamic cerebral autoregulation. However, as those differences are small in absolute values and as frequency domain measures which are of interest here appear to be quite similar (Panerai et al. 2006, 2008; Sammons et al. 2007), it is a reasonable approach to use the Finapres data for the comparisons performed here.

#### Inter-Method Agreement

The smoothed periodogram method and the two methods, i.e. the autoregressive-moving-average with exogenous inputs (ARMAX) and the vector-autoregressive (VAR) methods perform similar on the data set I in terms of distribution of the phase parameters. Similar figures for the smoothed periodogram method only have been reported (Reinhard et al. 2003, Table 2). Due to the technical advantages of parametric methods, and their ability to perform adaptive parameter estimation, they could be a central part of future diagnosis devices, which are able to deliver results online, without time delay due to block processing. Such a measurement device could be of value for monitoring of acutely ill patients in an intensive care unit.

#### Sampling Rate and Model Complexity

It was observed that for higher sampling rates the performance of the parametric approaches deteriorates. An explanation for this is that the parametric estimators need to model the transfer function over the whole frequency range intrinsically, while for the smoothed periodogram approach only the relevant frequency range 0.06–0.12 Hz (M-wave band) needs to be evaluated. Thus, the sampling rate of the raw data has been lowered to 2.5 Hz, which has been shown to be optimal in the sense that no influence of the phase estimates on the sampling rate between 2 and 4 Hz has been observed. For the smoothed periodogram approach, no dependence of the phase parameter on the sampling rate has been noticed up to a minimum sampling

rate of 1 Hz. Note that in (Panerai et al. 2003) a comparable sampling rate of 1.67 Hz has been used.

The ARMAX model exhibits the lowest complexity, while the VAR method and the smoothed periodogram method need a larger amount of model parameters. Although the smoothed periodogram method is able to select only frequencies of interest and neglects the others completely, it needs the highest number of model parameters. For the smoothed periodogram method it is necessary to design a taper window, whose shape and length need to be tuned a priori. In contrast, both parametric methods rely on objective parameter and order estimation criteria and thus they allow for a fully automated measurement procedure of the CAR functionality.

Regarding technical and practical applicability, the minimum data length for analysis of CAR is of importance. The minimal data length prescribes the maximum frequency resolution, which is available for the phase averaging (cf. Eq. 2) and it thus has to be bounded below. The frequency range of interest during spontaneous oscillations, 0.06–0.12 Hz, has the width of a full octave and should therefore be resolved in more detail. The frequency resolution is thus bounded by  $\Delta f \ll 0.06$  Hz, the minimum block length  $N_{\min}$  becomes  $N_{\min} \gg f_s/0.06 \approx 16f_s$ . For a sufficient frequency resolution, as needed for the frequency-averaging of spontaneous hemodynamic oscillations, the measurement time needs to be much larger than  $T_{\min} \approx 16$  s and it is independent of  $f_s$ . For much shorter time intervals than 16 s, the SPO phase parameters cannot be computed by frequency averaging as defined in Eq. 2 but they become an estimate based on a single frequency bin. We have shown that measurement of CAR based on spontaneous oscillations can be done with a data minimum length of  $N = 12,000$  corresponding to 12 s. Block-based processing schemes, as discussed in here, will introduce a delay in the range of 10–20 s. For parametric models various adaptive estimation schemes are available, which have the potential to lower this delay time substantially, thus making an online measurement procedure possible. A true online processing with a delay smaller than some seconds can be of great interest in (1) intensive online monitoring, and in (2) measurement protocols with changing paradigms such as deep breathing and spontaneous breathing interlaced.

#### Measurement Reproducibility

We showed that the phase parameter defined in Eq. 5 can be measured in a reproducible way on even data set II. From the scatter plots in Fig. 5 one can see that the performance is excellent for short-time reproducibility and it is also highly significant for the long-time reproducibility. Previous studies on reproducibility of CAR measurements

showed similar results but using other measurement setups. In (Smielewski et al. 1996) the transient hyperemic response test, i.e. inducing changes in middle cerebral artery blood flow velocity by brief ipsilateral carotid artery compressions of several seconds was compared to the thigh cuff test. The reproducibility of the transient hyperemic response ratio was more consistent than for the autoregulation index from the thigh cuff experiment. Another classical measurement setup, the lower body negative pressure box has been used to perform another study on reproducibility based on an eight-fold of measurements (Birch et al. 2002). In each session, a 12 s cycle has been applied to the person for a duration of 5 min and from ABP and CBFV the phase relationship has been estimated. Analyzing the deviation from the mean showed that the measurements are very reproducible. In (Liu et al. 2005) a reproducibility study based on the ARI was presented on a relatively small data set. It was concluded that data with too small variability in ABP shall be excluded from processing. However, we conclude that with our frequency-domain approaches the exclusion of weaker patients can be done automatically by estimating the coherence between ABP and CBFV. Finally, in Reinhard et al. (2003) the reproducibility for both deep breathing and spontaneous oscillations have been investigated, where for deep breathing at 0.1 Hz a higher significance has been shown because of univocal phase determination at 0.1 Hz. Interestingly, in that study, the phase from spontaneous oscillations was manually extracted from the point of maximum coherence within the low-frequency band, while in the present study automated extraction of phase was done by averaging phase values over all frequency bins exhibiting a significant coherence within the low-frequency band. The better reproducibility found with the presented procedure suggests that manual extraction of single phase values may be less adequate for phase estimation from spontaneous hemodynamic oscillations. We conclude that using averaged phase extraction also spontaneous oscillations can be used for reliable CAR measurement. The advantage of spontaneous oscillations is that no special patient compliance is needed.

## Conclusions

The two parametric approaches are valid alternatives to the smoothed periodogram method, and they are suitable for automatic assessment of cerebral autoregulation (CAR) with lower model complexity. It has also been shown that CAR measurement based on spontaneous oscillations can be a valid diagnostic tool. Thus the proposed methods as well as the classical method are useful for clinical monitoring of patients. The parametric estimators can be applied

in an adaptive real-time manner with minimum delay time. Especially the VAR approach is due to its very low minimum data length an attractive alternative for future monitoring applications. We also have shown that reproducibility of CAR measurement is highly significant, even for the case of repeated measurements within several months.

**Acknowledgements** We would like to thank M. Wolkewitz, H. Binder, J. Beyersmann, and A. Buller for stimulating discussions on statistical evaluation. This work was supported by the German Federal Ministry of Education and Research (01GQ0420) and the German Science Foundation (Ti315/4-2, He1949/1-1), and by the Excellence Initiative of the German Federal and State Governments.

## References

- Birch AA, Neil-Dwyer G, Murrills AJ. The repeatability of cerebral autoregulation assessment using sinusoidal lower body negative pressure. *Physiol Meas.* 2002;23:73–83.
- Brockwell PJ, Davis RA. *Time series: theory and methods.* Springer: NewYork; 1998.
- Choi BS. *ARMA model identification.* Springer; 1992.
- Diehl RR, Linden D, Lücke D, Berlit P. Phase relationship between cerebral blood flow velocity and blood pressure. *Stroke.* 1995;26:1801–4.
- Diehl RR, Linden D, Lücke D, Berlit P. Spontaneous blood pressure oscillations and cerebral autoregulation. *Clin Auton Res.* 1998;8:7–12.
- Hannan EJ, Deistler M. *The statistical theory of linear systems.* New York: Wiley; 1988.
- Kay SM. *Modern spectral estimation.* Englewood Cliffs, NJ: Prentice Hall; 1988.
- Liu Y, Allen R. Analysis of dynamic cerebral autoregulation using an ARX model based on arterial blood pressure and middle cerebral artery velocity simulation. *MBEC.* 2002;40:600–5.
- Liu J, Simpson DM, Allen R. High spontaneous fluctuation in arterial blood pressure improves the assessment of cerebral autoregulation. *Physiol Meas.* 2005;26:725–41.
- Ljung L. *System identification: theory for the user.* Englewood Cliffs: Prentice Hall; 1987.
- Matsukawa S, Wada T. Vector autoregressive modeling for analyzing feedback regulation between heart rate and blood pressure. *Am J Physiol Heart Circ Physiol* 1997;273:H478–86.
- Neumaier A, Schneider T. Estimation of parameters and eigenmodes of multivariate autoregressive models. *ACM Trans Math Softw* 2001;27:27–57.
- Panerai RB. Assessment of cerebral pressure autoregulation in humans—a review of measurement methods. *Physiol Meas.* 1998;19:305–38.
- Panerai RB. Cerebral autoregulation: from models to clinical applications. *Cardiovasc Eng.* 2008;8:42–59.
- Panerai RP, Dawson SL, Eames PJ, Potter JF. Cerebral blood flow velocity response to induced and spontaneous sudden changes in arterial blood pressure. *Am J Physiol Heart Circ Physiol* 2001; 280:H2162–74.
- Panerai RB, Eames PJ, Potter JF. Variability of time-domain indices of dynamic cerebral autoregulation. *Physiol Meas.* 2003;24:367–81.
- Panerai RB, Sammons EL, Smith SM, Rathbone WE, Bentley S, Potter JF, Evans DH, Samani NJ. Cerebral critical closing pressure estimation from Finapres and arterial blood pressure measurements in the aorta. *Physiol Meas.* 2006;27:1387–402.

- Panerai RB, Sammons EL, Smith SM, Rathbone WE, Bentley S, Potter JF, Samani NJ. Continuous estimates of dynamic cerebral autoregulation: influence of non-invasive arterial blood pressure measurements. *Physiol Meas*. 2008;29:497–513.
- Reinhard M, Müller T, Guschlbauer B, Timmer J, Hetzel A. Transfer function analysis for clinical evaluation of dynamic cerebral autoregulation—a comparison between spontaneous and respiratory-induced oscillations. *Physiol Meas*. 2003;24:27–43.
- Sammons EL, Samani NJ, Smith SM, Rathbone WE, Bentley S, Potter JF, Panerai RB. Influence of noninvasive peripheral arterial blood pressure measurements on assessment of dynamic cerebral autoregulation. *J Appl Physiol*. 2007;103:369–75.
- Schneider T, Neumaier A. Algorithm 808: ARfit—A Matlab package for the estimation of parameters and eigenmodes of multivariate autoregressive models. *ACM Trans Math Softw*. 2001;27:58–65.
- Smielewski P, Czosnyka M, Kirkpatrick P, McEroy H, Rutkowska H, Pickard JD. Assessment of cerebral autoregulation using carotid artery compression. *Stroke*. 1996;27:2197–203.
- Tiecks FP, Lam AM, Aaslid R, Newell DW. Comparison of static and dynamic autoregulation measurements. *Stroke* 1995;26:1014–9.
- Zhang R, Zuckerman JH, Giller CA, Levine BD. Transfer function analysis of dynamic cerebral autoregulation in humans. *Am J Physiol* 1998;274:H233–41.